

An Inner/Outer Loop Controller for Rigid-Flexible Manipulators¹

F. Khorrami

School of Electrical Engineering &
Computer Science,
Polytechnic University,
Brooklyn, NY 11201

S. Zheng

AT&T Bell Laboratories,
Middletown, NJ 07748

In this paper, vibration control of flexible-link manipulators is considered. A nonlinear partial differential equation describing the dynamics of a two-link planar manipulator with a flexible forearm is derived. Thereafter, utilizing the eigenfunctions corresponding to the boundary value problem at hand, a finite-dimensional approximation of the model is given. The controller design strategy is based upon an inner-loop controller which corresponds to the rigid body motion of the manipulator taking into consideration the vibrations of the manipulator and an outer-loop controller for further vibration damping and robustness enhancement of the closed-loop dynamics to parameter variations in the system. The measurement used in the outer-loop controller is obtained through an accelerometer mounted on the flexible forearm which can be easily attained in an experimental setup. The control methodology advocated in this paper are applicable to the multi-link flexible manipulators.

I Introduction

Due to earth-based and space-based applications, much attention has been given to modeling and control of flexible-link manipulators. The use of lightweight manipulators stems from their lower mass, higher mobility, reduced energy consumption, smaller actuators, etc. One example is the RMS that has been designed for assembling tasks of the space station. Furthermore, studies on articulated elastic multi-body systems also enhance the knowledge in Control/Structure Interaction of large space structures.

The literature is voluminous of research on modeling of flexible-link manipulators. Different approaches such as finite element method, Hamiltonian, and Newtonian have been utilized to model manipulators with non-rigid links [1–5]. Many models with different degrees of complexity have been introduced in the literature, i.e., some or all terms corresponding to Coriolis, shear, torsion, axial displacement, gravity, and centrifugal stiffening have been neglected.

The complication in controller synthesis for multi-link flexible manipulators is due to the fact that the input/state map of flexible-link manipulators is not externally feedback linearizable [6–8]. In addition, the dynamics of flexible-link manipulators are much more complicated than the corresponding rigid-link manipulators. Not only the distributed parameter nature of the dynamics is a complication, but also the moving boundary conditions at the tip of the flexible links connected to the next link is a major difficulty.

Several experimental results have been presented in the lit-

erature for single-link flexible manipulators [9–13]. Recently, experimental results on two-link flexible manipulators have been reported [14–17]. At this point, most of the experimental work has been focused on a rigid-flex manipulator (i.e., first link rigid and second link flexible). Furthermore, almost all the controller designs have been based upon finite-dimensional approximations of the dynamics.

Perturbation methods have been shown to be promising in dealing with flexible manipulators. Khorasani and Spong [18, 19] have decomposed the dynamic of a manipulator with flexibility at joints into two subsystems, *slow* and *fast*. The slow subsystem corresponded to the rigid body movement and the fast subsystem was comprised of the elastic forces at joints. Siciliano et al. [20] have pursued a singular perturbation approach for flexible-link arms. In that work, the dynamics of the manipulator have been taken as a finite set of ordinary differential equations. Khorrami et al. [21, 5] performed an asymptotic expansion on the integro-partial differential equations describing the dynamics of multi-link flexible manipulators. This approach will be briefly outlined in the sequel.

In this paper, an inner-loop nonlinear feedback controller is designed first. At the second stage, an outer-loop controller is applied for suppression of vibration due to the rigid body motion and also to enhance the robustness of the controller to parameter variations in the system. The inner-loop controller is based on the asymptotic expansion techniques reported earlier [21, 5]. In the inner-loop design, the $\mathcal{O}(1)$ terms in the dynamics are feedback linearized and also the vibrations induced on the links by this controller are taken into consideration. The outer-loop design is an *output feedback linear quadratic design* which reduces to a nonconvex optimization problem. In the next sections, the dynamics of the flexible-link manipulators are derived and a finite dimensional approximation for the outer-loop design is given.

¹This paper was presented at the 1990 American Control Conference, San Diego, CA.

Contributed by the Dynamic Systems and Control Division for publication in the JOURNAL OF DYNAMIC SYSTEMS, MEASUREMENTS, AND CONTROL. Manuscript received by the Dynamic Systems and Control Division July 24, 1991; revised manuscript received March 1992. Associate Technical Editor: J. Bentsman.

II Modeling of Open Kinematic Chain Flexible-Link Robot Manipulators

In this section, a detailed derivation of the dynamics for open chain kinematic flexible manipulators is presented. The approach advocated is the extended Hamilton principle. Various effects such as axial displacement, shear, torsion, centrifugal stiffening, Coriolis, and gravity are explained and considered. The dynamical equations for a two-link planar manipulator with a flexible forearm (a hybrid manipulator) are given. As mentioned previously, different approaches with different assumptions have been reported in modeling of flexible-link manipulators [1-5].

The following are the parameters of the manipulator and the notation used hereafter:

Figure 1 depicts a two-link flexible manipulator. The notation used below is also demonstrated in Fig. 1.

The extended Hamiltonian is given by

$$H = T + W \quad (1)$$

where T and W are the kinetic energy and work function of the arm respectively.

The dynamical equations of multi link flexible manipulators are obtained by the principle of least action in the following manner:

$$\delta \left(\int_{t_0}^{t_f} H dt \right) = 0 \quad (2)$$

where $\delta(\cdot)$ represents the first variation of (\cdot) .

In the next subsections, the kinetic and potential (work) energies are formulated.

A. Kinetic Energy. The kinetic energy of the flexible manipulator is composed of the following terms:

kinetic energy due to hub

$$\frac{1}{2} I_h \dot{\theta}_1^2$$

kinetic energy due to link i

$$\frac{1}{2} \int_{m_i} \dot{\mathbf{R}}_i \cdot \dot{\mathbf{R}}_i dm_i$$

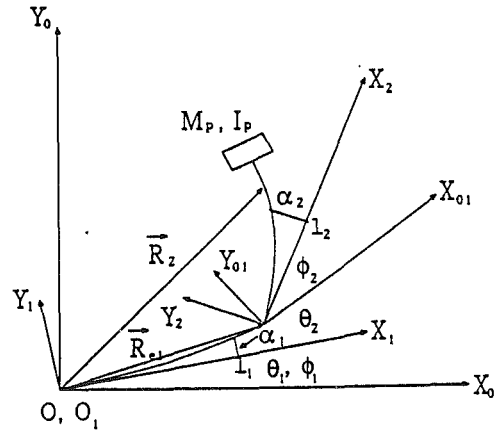


Fig. 1 A two-link flexible manipulator

kinetic energy due to mass M_i at O_i

$$\frac{1}{2} M_i \dot{\mathbf{R}}_{e_i} \cdot \dot{\mathbf{R}}_{e_i}$$

kinetic energy due to M_i inertia

$$\frac{1}{2} I_i \dot{\xi}_i^2; \quad \xi_i = \sum_{j=1}^i \dot{\theta}_j + \sum_{j=1}^{i-1} \left(\frac{\partial \alpha_i}{\partial t_j} \Big|_{l_i=L_j} \right)^2$$

Therefore, the total kinetic energy of the system is

$$T = \frac{1}{2} I_h \dot{\theta}_1^2 + \sum_{i=1}^n \frac{1}{2} \left[M_i \dot{\mathbf{R}}_{e_i} \cdot \dot{\mathbf{R}}_{e_i} + I_i \dot{\xi}_i^2 + \int_{m_i} \dot{\mathbf{R}}_i \cdot \dot{\mathbf{R}}_i dm_i \right] \quad (3)$$

To evaluate the terms appearing in Eq. (3), the position vector \mathbf{R}_i needs to be evaluated. Consider $\alpha_i(l_i, t)$ which represents the deflection of the link from its rigid shape in the coordinate frame $O_i X_i Y_i$. The vector position \mathbf{R}_i in the i th frame is given as

$$\mathbf{R}_i = l_i e_{x_i} + \alpha_i(l_i, t) e_{y_i} = \{E_i\}^T \begin{pmatrix} l_i \\ \alpha_i \end{pmatrix}$$

where $(\cdot)^T$ denotes transpose of (\cdot) , e_{x_i} and e_{y_i} are the unit vectors in frame i .

To write \mathbf{R}_i in the inertial frame, consider

Nomenclature

I_h = hub inertia	I_p = payload inertia with respect to its center of mass ($I_p = I_n$)
L_i = length of link i	$\{E_i\}$ = the unit vector for coordinate frame $\{O_i X_i Y_i\}$
E_i = Young's modulus of link i	$\{E_0\}$ = the unit vector in the inertial coordinate frame
ρ_i = mass density of link i	T_i = the coordinate transform from i th coordinate to the inertial frame
I_i = area moment of inertia of link i	h_i = axial displacement for link i
m_i = mass of link i	β_i = the angle of distortion due to shear for link i
A_i = cross sectional area of link i	ψ_i = the angle of rotation due to bending for link i
l_i = the spatial variable for link i	\mathbf{R}_i = position vector for link i
$\alpha_i(l_i, t)$ = the deviation of the link from X_i at position l_i	\mathbf{R}_{e_i} = position vector corresponding to the end point of link i
$O X_0 Y_0$ = inertial coordinate frame	θ_i = the angle between X_i and X_{i-1}
$O_i X_i Y_i$ = moving coordinate frame with origin at the hub of link i ; X_i is tangent to link i at O_i	φ_{i+1} = the angle between X_{0i} and X_{i+1} ; $\varphi_1 = \theta_1$
$O_{0i} X_{0i} Y_{0i}$ = moving coordinate frame with origin at the tip of link i X_{0i} is the tangent to the tip at link i	g = gravitational constant
M_i = mass at O_i	u_i = the input torque at joint i
I_i = inertia of mass at O_i with respect to its center of mass	G_i = shear modulus of link i
M_p = payload mass ($M_p = M_n$)	K'_i = a constant depending on the shape of the i th link cross-section

$$\mathbf{R}_i = \mathbf{R}_{e_{i-1}} + T_i \begin{pmatrix} l_i \\ \alpha_i(l_i, t) \end{pmatrix}; \quad i=2, \dots, n, \quad (4)$$

$$\mathbf{R}_{e_i} = \mathbf{R}_i \Big|_{l_i=L_i}; \quad i=1, \dots, n$$

Therefore, \mathbf{R}_i in the inertial coordinate frame is given by

$$\mathbf{R}_i = \{E_0\}^T \left\{ T_{i-1} \begin{pmatrix} L_{i-1} \\ \alpha_{i-1}(L_{i-1}, t) \end{pmatrix} + T_i \begin{pmatrix} l_i \\ \alpha_i(l_i, t) \end{pmatrix} \right\}. \quad (5)$$

The above analysis yields the kinetic energy for n -link open kinematic chain flexible manipulators. The dynamics of two-link manipulators with a flexible forearm are given in a later section.

B. The Work Function. The total work function is

$$W = W_c + W_{nc}$$

where W_c and W_{nc} are the conservative and nonconservative work functions.

The conservative forces in a system are derivable from a potential function. However, the non-conservative forces change the energy of a particle. These forces such as external forces and friction are energy dissipating.

The conservative work is comprised of

- strain energy,
- shear energy,
- tension-compression energy,
- centrifugal stiffening.

The strain energy of an elastic material is analogous to the energy stored in a spring and the potential energy arising from strain energy is

$$\frac{1}{2} \int_0^{L_i} E_i I_i \psi_{i,i}^2 dl_i. \quad (6)$$

The potential energy due to shear is

$$\frac{1}{2} \int_0^{L_i} K_i' G_i A_i \beta_i^2 dl_i, \quad (7)$$

and for tension-compression, energy is

$$\frac{1}{2} \int_0^{L_i} E_i A_i h_{i,i}^2 dl_i. \quad (8)$$

Finally, the potential energy from the centrifugal stiffening has the form

$$\frac{1}{2} \rho_i \int_0^{L_i} (L_i^2 - l_i^2) \dot{\theta}_i^2 y_{i,i}^2 dl_i. \quad (9)$$

The nonconservative work done by the external torques at the joints is

$$W_{nc} = \sum_{i=2}^n u_i \left(\theta_i - \frac{\partial \alpha_{i-1}}{\partial l_{i-1}} \Big|_{l_{i-1}=L_{i-1}} \right) + u_1 \theta_1$$

$$= \sum_{n=1}^{\infty} u_i \varphi_i + u_1 \varphi_1. \quad (10)$$

From the above discussion, one can form the total work function ($W = W_c + W_{nc} = -V + W_{nc}$, where V is the potential energy). Many of the above terms have been neglected in almost all previous studies especially for controller designer purposes. The most important and dominating term in the potential energy is the strain energy; however, depending on the nature of the application and problem at hand, the rest of the terms may be neglected. The generalized coordinates for the rigid body may be taken either as θ_i or φ_i .

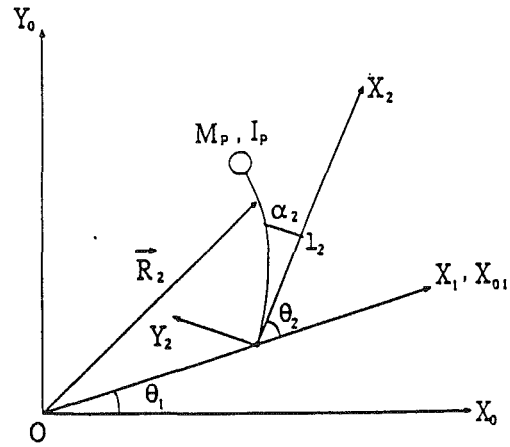


Fig. 2 A hybrid manipulator

In the following analysis, we only consider the rigid body and the transverse motion dynamics, i.e., we assume that the shear and the axial displacements are negligible. However, nonlinearities that arise from centripetal forces, Coriolis, and gravity will be accounted for.

III Dynamics of a Hybrid Manipulator

In this section, a two-link manipulator with a flexible forearm (a hybrid manipulator) is considered (Fig. 2). Utilizing the expressions for the energy terms derived in the previous section and the Hamiltonian principle, the dynamics are obtained. The details of the derivation are omitted here.

The dynamical equations in this case are as follows:

The first link rigid body motion (θ_1):

$$\left[I_h + \frac{1}{3} \rho_1 L_1^3 + \rho_2 L_1^2 L_2 + \frac{1}{3} \rho_2 L_2^3 + \rho_2 L_1 L_2^2 \cos \theta_2 \right. \\ \left. - 2 \rho_2 L_1 \sin \theta_2 \int_0^{L_2} \alpha_2 dl_2 + \rho_2 \int_0^{L_2} \alpha_2^2 dl_2 \right] \ddot{\theta}_1 \\ + \left[\frac{1}{3} \rho_2 L_2^3 + \frac{1}{2} \rho_2 L_1 L_2^2 \cos \theta_2 - \rho_2 L_1 \sin \theta_2 \int_0^{L_2} \alpha_2 dl_2 \right. \\ \left. + \rho_2 \int_0^{L_2} \alpha_2^2 dl_2 \right] \ddot{\theta}_2 + \rho_2 \int_0^{L_2} (l_2 + L_1 \cos \theta_2) \ddot{\alpha}_2 dl_2 = u_1 \\ + \rho_2 L_1 \int_0^{L_2} [(l_2 \sin \theta_2 + \alpha_2 \cos \theta_2) (\dot{\theta}_2^2 + 2 \dot{\theta}_1 \dot{\theta}_2)] dl_2 \\ + 2 \rho_2 L_1 (\dot{\theta}_1 + \dot{\theta}_2) \sin \theta_2 \int_0^{L_2} \dot{\alpha}_2 dl_2 - 2 \rho_2 (\dot{\theta}_1 + \dot{\theta}_2) \int_0^{L_2} \alpha_2 \dot{\alpha}_2 dl_2 \\ + \rho_2 g \int_0^{L_2} [L_1 \cos \theta_1 + l_2 \cos(\theta_1 + \theta_2) + \alpha_2 \sin(\theta_1 + \theta_2)] dl_2 \quad (11)$$

The second link rigid body motion (θ_2):

$$\rho_2 \left[\frac{1}{3} L_2^3 + \frac{1}{2} L_1 L_2^2 \cos \theta_2 - L_1 \sin \theta_2 \int_0^{L_2} \alpha_2 dl_2 + \int_0^{L_2} \alpha_2^2 dl_2 \right] \ddot{\theta}_1 \\ + \left[\frac{1}{3} \rho_2 L_2^3 + \rho_2 \int_0^{L_2} \alpha_2^2 dl_2 \right] \ddot{\theta}_2 + \rho_2 \int_0^{L_2} l_2 \ddot{\alpha}_2 dl_2 \\ = -\frac{1}{2} \rho_2 L_1 L_2^2 \dot{\theta}_1^2 \sin \theta_2 \\ - \rho_2 L_1 \dot{\theta}_1^2 \cos \theta_2 \int_0^{L_2} \alpha_2 dl_2 - 2 \rho_2 (\dot{\theta}_1 + \dot{\theta}_2) \int_0^{L_2} \alpha_2 \dot{\alpha}_2 dl_2 \\ + \rho_2 g \int_0^{L_2} [l_2 \cos(\theta_1 + \theta_2) + \alpha_2 \sin(\theta_1 + \theta_2)] dl_2 + u_2 \quad (12)$$

The transverse motion (flexure) of the second link (α_2):

$$\begin{aligned} \rho_2 I_2 (\ddot{\theta}_1 + \ddot{\theta}_2) + \rho_2 \ddot{\alpha}_2 + \rho_2 L_1 \ddot{\theta}_1 \cos \theta_2 = & -E_2 I_2 \alpha_2 l_2 l_2 l_2 l_2 \\ & - \rho_2 (L_1 \sin \theta_2 - \alpha_2) \dot{\theta}_1^2 + \rho_2 \alpha_2 \dot{\theta}_2^2 + 2\rho_2 \dot{\theta}_1 \dot{\theta}_2 \alpha_2 \\ & + \rho_2 g \cos (\theta_1 + \theta_2) \end{aligned} \quad (13)$$

with the following boundary conditions

$$\alpha_2(0, t) = 0 \quad (14a)$$

$$\frac{\partial}{\partial l} \alpha_2(0, t) = 0 \quad (14b)$$

$$\frac{\partial^2}{\partial l^2} \alpha_2(L, t) = 0 \quad (14c)$$

$$\frac{\partial^3}{\partial l^3} \alpha_2(L, t) = 0 \quad (14d)$$

and initial conditions

$$\alpha_2(l, 0) = \alpha_0(l) \quad , l \in [0, L] \quad (15a)$$

$$\frac{\partial}{\partial t} \alpha_2(l, 0) = \dot{\alpha}_0(l) \quad , l \in [0, L] \quad (15b)$$

$$\underline{\theta}(0) = \underline{\Theta}_0 \quad (15c)$$

$$\underline{\dot{\theta}}(0) = \underline{\dot{\Theta}}_0 \quad (15d)$$

Remark 1: (14c) and (14d) are due to the absence of bending moment and shearing forces respectively at the tip of the link. Addition of a payload mass and inertia will change these boundary conditions [3]. For brevity, the payload effects are neglected; although, they are included in the simulations studies.

IV Finite-Dimensional Approximation

The flexible-link manipulators are distributed parameter (continuous) systems. If the models are to be used in simulation studies and controller design, due to actuator/sensor bandwidth limits it is rather reasonable to retain a truncated model representing the system at the lower frequencies. To this end, the system needs to be approximated by a finite-dimensional model which ignores the high-frequency modes.

There exist different techniques to discretize a continuous system. The basic idea is to approximate the distributed parameter by a finite set of trial functions. In our case, the flexure variable, $\alpha_2(l_2, t)$, is to be approximated as follows:

$$\alpha_2(l_2, t) = \sum_{j=1}^p \eta_j(t) \Phi_j(l_2) \quad (16)$$

The choice of functions $\Phi_j(l_2)$ is rather crucial. The best way to choose this set of functions is to use the eigenfunctions that arise from the linearized problem at hand. If the eigenfunctions are used, the expansion (16) is known as the unconstrained mode expansion. However, for all practical purposes solving the eigenvalue problem for the system at hand may not be easy, even impossible. Therefore, to pursue discretization of the system, a set of functions need to be chosen. The approximation known as the Ritz-Kantorovich method employs a "complete set of functions." This technique is also known as the "assumed mode" method or constrained mode expansion.

The trial functions in this case are obtained by fixing the rigid body motion and setting the external inputs to zero. Therefore, the dynamics given in (13) reduces to the dynamics of an Euler-Bernoulli beam, i.e.,

$$\alpha_{tt} = -\frac{EI}{\rho} \alpha \quad (17)$$

where A is a linear operator, i.e., $A = d^4/dx^4$.

In this case, the following eigenvalue problem needs to be solved

$$A\Phi = \lambda\Phi, \quad (18)$$

subject to

$$\Phi(0) = \Phi^{(1)}(0) = \Phi^{(2)}(L) = \Phi^{(3)}(L) = 0$$

where $(\cdot)^{(i)}$ denotes the i th derivative of (\cdot) .

It is well-known [22] that the solution of the above eigenvalue problem is

$$\Phi_i(l) = \cosh(\gamma_i l) - \cos(\gamma_i l) - \xi_i [\sinh(\gamma_i l) - \sin(\gamma_i l)] \quad (19a)$$

where

$$\xi_i = \frac{\cosh(\gamma_i L) + \cos(\gamma_i L)}{\sinh(\gamma_i L) + \sin(\gamma_i L)} \quad (19b)$$

and γ_i 's satisfy

$$\cos(\gamma_i L) \cosh(\gamma_i L) = -1. \quad (19c)$$

Remark 2: The eigenfunctions given by (19a) are pairwise orthogonal, i.e., $\langle \Phi_i, \Phi_k \rangle = L\delta_{ik}$ where δ is the dirac delta and $\langle \cdot, \cdot \rangle$ denotes the inner product.

Choosing the first p eigenfunctions (mode-shapes) given by (19a) as the assumed modes for the discretization process, the following lumped representation of the system is obtained²:

$$\mathfrak{M}\dot{X} + KX = F(X, \dot{X}) + G(X) + Bu \quad (20)$$

where $X = [\theta_1 \ \theta_2 \ \eta_1 \ \eta_2 \ \dots \ \eta_p]^T$, \mathfrak{M} , K , F , G , and B are the inertia, stiffness, vector of nonlinearities due to Coriolis and centripetal forces, gravity, and input matrix, respectively, and are given in the Appendix. We consider the motion in the horizontal plane; therefore, $g = 0$ (i.e., no gravity terms).

V Controller Design

The controller advocated in this paper is based upon an inner-loop/outer-loop design. The inner-loop controller is a nonlinear feedback law derived from the asymptotic expansion analysis performed on the distributed parameter dynamics of the hybrid manipulator. The outer-loop is a linear output feedback designed according to a quadratic cost criterion. The output feedback problem is solved through a nonlinear optimization approach. In the next subsections, the inner-loop and outer-loop controllers are presented.

A. Inner-Loop Controller. A multi-parameter asymptotic expansion analysis of the dynamics of the multi-link flexible manipulators has been given [5, 21, 23]. Utilizing this approach, an inner-loop controller is established. For completeness, a brief derivation of the terms in the asymptotic expansion is given here. For brevity, we will ignore the gravity terms.³

Consider the following nondimensional parameters

$$y = \frac{\alpha_2}{L_2}, \quad x_2 = \frac{l_2}{L_2} \quad (21)$$

$$\hat{u}_1 = \frac{1}{\rho_2 L_1^3} u_1 \quad (22)$$

$$\hat{u}_2 = \frac{1}{\rho_2 L_1 L_2^2} u_2 \quad (23)$$

$$J = \frac{1}{3} + \frac{I_h}{\rho_1 L_1^3} + \frac{\rho_2 L_2}{\rho_1 L_1} + \frac{\rho_2 L_2^3}{3\rho_1 L_1^3} \quad (24)$$

²Other sets of functions that satisfy the geometric boundary conditions may also be utilized, i.e., the mode-shapes corresponding to the clamped-mass boundary conditions or functions approximating the static deformations of the beam.

³Inclusion of the gravity term can be handled similarly by modification of the perturbation parameter as shown in [21] and it does not change the scope of the problem at hand.

$$\rho = \frac{\rho_2}{\rho_1}, \quad L = \frac{L_2}{L_1} \quad (25)$$

Using the above parameters, the dynamics may be rewritten as follows:

The first link rigid body motion (θ_1):

$$\begin{aligned} & \left[J + \rho L^2 \cos \theta_2 - 2\rho L^2 \sin \theta_2 \int_0^1 y dx + \rho L^3 \int_0^1 y^2 dx \right] \ddot{\theta}_1 \\ & + \left[\frac{1}{3} \rho L^3 + \frac{1}{2} \rho L^2 \cos \theta_2 - \rho L^2 \sin \theta_2 \int_0^1 y dx + \rho L^3 \int_0^1 y^2 dx \right] \ddot{\theta}_2 \\ & + \rho L^2 \int_0^1 (Lx + \cos \theta_2) \ddot{\alpha}_2 dx = \hat{u}_1 \\ & + \rho L^2 \int_0^1 [(x \sin \theta_2 + y \cos \theta_2)(\dot{\theta}_2^2 + 2\dot{\theta}_1 \dot{\theta}_2)] dx \\ & + 2\rho L^2 (\dot{\theta}_1 + \dot{\theta}_2) \sin \theta_2 \int_0^1 y dx - 2\rho L^3 (\dot{\theta}_1 + \dot{\theta}_2) \int_0^1 y y dx \quad (26) \end{aligned}$$

The second link rigid body motion (θ_2):

$$\begin{aligned} & \left[\frac{1}{3} L + \frac{1}{2} \cos \theta_2 - \sin \theta_2 \int_0^1 y dx + L \int_0^1 y^2 dx \right] \ddot{\theta}_1 \\ & + \left[\frac{1}{3} L + L \int_0^1 y^2 dx \right] \ddot{\theta}_2 + L \int_0^1 x y \ddot{\alpha}_2 dx = \hat{u}_2 - \frac{1}{2} \dot{\theta}_1^2 \sin \theta_2 \\ & - \dot{\theta}_1^2 \cos \theta_2 \int_0^1 y dx - 2L (\dot{\theta}_1 + \dot{\theta}_2) \int_0^1 y y dx \quad (27) \end{aligned}$$

The transverse motion (flexure) of the second link (α_2):

$$\begin{aligned} x(\ddot{\theta}_1 + \ddot{\theta}_2) + \ddot{y} + \frac{1}{L} \ddot{\theta}_1 \cos \theta_2 = -\omega_f^2 y_{xxxx} \\ - \left(\frac{1}{L} \sin \theta_2 - y \right) \dot{\theta}_1^2 + y \dot{\theta}_2^2 + 2\dot{\theta}_1 \dot{\theta}_2 y \quad (28) \end{aligned}$$

where

$$\omega_f^2 = \frac{E_2 I_2}{\rho_2 L_2^4} \quad (29)$$

A perturbation parameter, namely ϵ , may be embedded in the dynamics through the term ω_f^2 . Choosing this quantity as $\mathcal{O}(1/\epsilon)$ implies that as the link becomes shorter or as the bending stiffness of the link becomes larger, the perturbation parameter becomes smaller. In turn, this corresponds to the fact that as this parameter vanishes the manipulator behaves as if it were rigid. It was shown [5, 21] that the flexure variable was of order ϵ .

Utilizing the invariant manifold theory and expanding the variables as follows

$$y = h = \epsilon h_0 + \epsilon^2 h_1 + \mathcal{O}(\epsilon^3) \quad (30)$$

$$u = u_0 + \epsilon u_1 + \mathcal{O}(\epsilon^2), \quad (31)$$

we obtain the following approximations to the manifold from (28):

$$\mathcal{O}(1): h_0,_{xxxx} = -x(\ddot{\theta}_1 + \ddot{\theta}_2) - \frac{1}{L} \ddot{\theta}_1 \cos \theta_2 - \frac{1}{L} \sin \theta_2 \dot{\theta}_1^2 \quad (32)$$

$$\mathcal{O}(\epsilon^k): h_k,_{xxxx} = -\ddot{h}_{k-1} + (\dot{\theta}_1 + \dot{\theta}_2)^2 h_{k-1}, \quad k \geq 1. \quad (33)$$

Equations (32)–(33) yield analytical solutions for the flexure variable up to any order of ϵ . This analytical representation of the vibration can be utilized in the controller design. Having obtained the approximations to the manifold, the approximations to the rigid body dynamics are attained by substituting the manifold solution in (26)–(27). The $\mathcal{O}(1)$ approximation to the rigid body dynamics is as follows:

The first link rigid body motion (θ_1):

$$\begin{aligned} & \left[J + \rho L^2 \cos \theta_2 \right] \ddot{\theta}_1 + \left[\frac{1}{3} \rho L^3 + \frac{1}{2} \rho L^2 \cos \theta_2 \right] \ddot{\theta}_2 \\ & = \frac{1}{2} \rho L^2 \sin \theta_2 (\dot{\theta}_2^2 + 2\dot{\theta}_1 \dot{\theta}_2) + \hat{u}_1^0 \quad (34) \end{aligned}$$

The second link rigid body motion (θ_2):

$$\left[\frac{1}{3} L + \frac{1}{2} \cos \theta_2 \right] \ddot{\theta}_1 + \frac{1}{3} L \ddot{\theta}_2 = -\frac{1}{2} \dot{\theta}_1^2 \sin \theta_2 + \hat{u}_2^0 \quad (35)$$

The $\mathcal{O}(1)$ rigid body dynamics can be linearized via the following nonlinear feedback control law:

$$\begin{aligned} \begin{bmatrix} \hat{u}_1^0 \\ \hat{u}_2^0 \end{bmatrix} &= \begin{bmatrix} J + \rho L^2 \cos \theta_2 & \frac{1}{3} \rho L^3 + \frac{1}{2} \rho L^2 \cos \theta_2 \\ \frac{1}{3} L + \frac{1}{2} \cos \theta_2 & \frac{1}{3} L \end{bmatrix} \begin{bmatrix} v_1 \\ v_2 \end{bmatrix} \\ &+ \begin{bmatrix} -\frac{1}{2} \rho L^2 \sin \theta_2 (\dot{\theta}_2^2 + 2\dot{\theta}_1 \dot{\theta}_2) \\ \frac{1}{2} \dot{\theta}_1^2 \sin \theta_2 \end{bmatrix} = D(\underline{\theta}) v + h(\underline{\theta}, \dot{\underline{\theta}}). \quad (36) \end{aligned}$$

where v_i s are the new inputs and may be chosen as the linear feedbacks of the form

$$v_i = -K_{i1}(\theta_i - \theta_{iref}) - K_{i2}(\dot{\theta}_i - \dot{\theta}_{iref}) + \ddot{\theta}_{iref}, \quad i = 1, 2. \quad (37)$$

The choice of feedback gains affects the speed of the maneuver and importantly the magnitude of vibrations on the links and the tip of the manipulator. The induced vibrations on the links by the rigid body motion can be estimated from the approximations to the manifold given by (32)–(33). This analytical representation of the vibrations may be utilized to choose the feedback gains. The control laws given by (36)–(37) are the so called inner-loop controller. The outer-loop controller will be added to v_i s.

B. Outer-Loop Controller.

Implementation of the inner-loop controller described in the previous section only requires the measurements of position and angular velocities of each link which are easy to measure (e.g., using optical encoders and DC tachometers). This controller will have satisfactory performance as long as the links are reasonably stiff and short. However, appreciable degradation in the performance of the inner loop controller occurs when the stiffness of the manipulator decreases and especially when the lengths of the flexible links increase. This can be seen from the perturbation parameter introduced earlier. The manipulator softens proportional to the cube of the length of the link and linearly with its stiffness.

To further enhance the performance and/or robustness of the system to parameter variations and payload changes, some measurements of the vibrations are necessary. To this end, we assume that the end-effector velocity (or acceleration) is available. This measurement can be implemented by mounting an accelerometer at the tip of the manipulator. There are also other available techniques to measure tip position and velocity of the arm such as: 1) a camera system, 2) ultrasonic ranging systems, 3) strain gages, and 4) laser position measuring systems. Furthermore, one may elect to use the accelerometer output signal directly. Thereafter, an output feedback based upon a quadratic performance is designed. As will be noticed in the simulations, this additional feedback enhances the performance and robustness of the closed-loop system.

The relative tip velocity in the local frame is given by $\dot{\alpha}(L_2, t)$. In terms of our finite-dimensional approximation of the system, this output measurement may be rewritten as

$$y_1 = C_1 z = [0 \dots 0 \ 1 \ 0 \ 0 \ \Phi_1(L_2) \dots \Phi_p(L_2)] z \quad (38)$$

where $z = [\tilde{x}^T \ \tilde{\dot{x}}^T]^T$ and $\tilde{x} = [\theta_1 - \theta_{1f} \ \theta_2 - \theta_{2f} \ \eta_1 \ \eta_2 \dots \eta_p]^T$ and

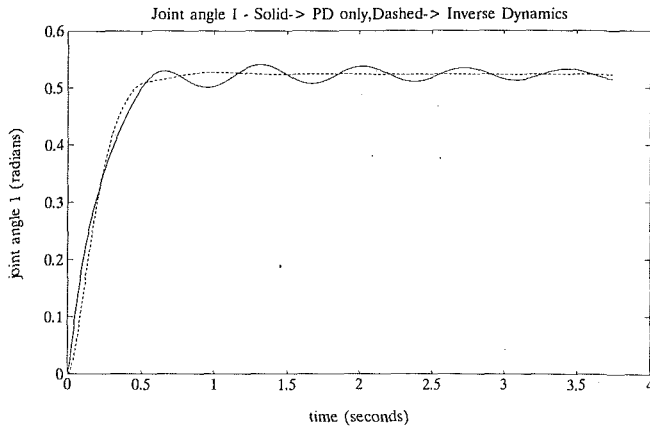


Fig. 3(a) The first joint angle, θ_1

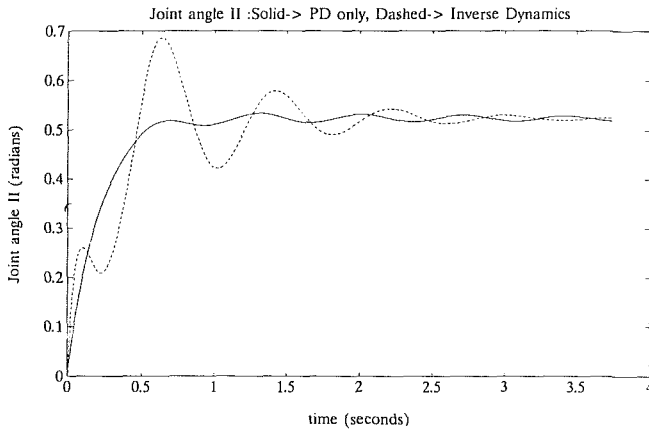


Fig. 3(b) The second joint angle, θ_2

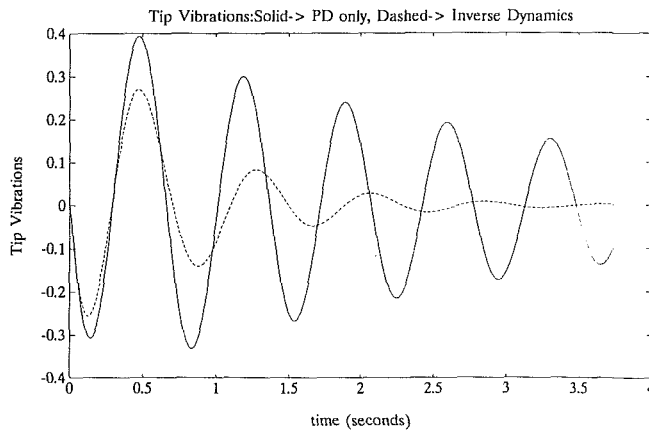


Fig. 3(c) Tip deflection, $\alpha_2(L_2, t)$

Fig. 3 Response of the arm under the PD and the inner-loop controller

θ_{if} ($i=1,2$) are the final (steady-state) values of the joint positions.

The outer-loop controller is designed based on a linear quadratic design. Therefore, the dynamics of the closed-loop system (i.e., including the inner-loop controller) is linearized around $z=0$. The linearized dynamics are denoted as

$$\dot{z} = \hat{A}z + \hat{B}w \quad (39)$$

$$y = \hat{C}z \quad (40)$$

where

$$\hat{A} = \begin{bmatrix} 0 & I \\ -M^{-1}[K + BD(X_e)K_1] & -M^{-1}[BD(X_e)K_2] \end{bmatrix} \quad (41)$$

$$\hat{B} = \begin{pmatrix} 0 \\ M^{-1}[BD(X_e)] \end{pmatrix} \quad (42)$$

$$K_i = \text{diag}(K_{1i}, K_{2i}), \quad i=1, 2, \quad (43)$$

and \hat{C} is the output matrix comprised of C_1 and possibly the joint positions and velocities and $X_e = [\theta_{1f} \theta_{2f} 0 \dots 0]^T$.

The output linear quadratic design is to minimize

$$\mathcal{J} = \frac{1}{2} \int_0^{\infty} (z^T Q z + w^T R w) dt \quad (44)$$

constraint to the following control structure:

$$w = K y. \quad (45)$$

It can be shown that the necessary conditions for minimizing \mathcal{J} given by (44) with the controller structure (45) imply the solution of the following system of nonlinear algebraic equations:

$$\begin{cases} A_c^T P + P A_c + \bar{Q} = 0 \\ A_c L + L A_c^T + X_0 = 0 \end{cases} \quad (46a)$$

and

$$\nabla_K \mathcal{J} = \hat{B}^T P L \hat{C}^T + \hat{R} K \hat{C} L \hat{C}^T = 0 \quad (46b)$$

where

$$A_c = \hat{A} + \hat{B} K \hat{C} \quad (47a)$$

$$\bar{Q} = \hat{Q} + \hat{C}^T K^T \hat{R} K \hat{C} \quad (47b)$$

$$X_0 = z(0) z^T(0). \quad (47c)$$

A large software package part of which solves the above non-convex optimization problem has been developed. The algorithm used to solve the output feedback problem is a gradient technique with a Fibonacci linear search for determination of the optimal step size. It is well known that the selection of the weights in the optimization procedure is not necessarily straightforward. Here, we tried to penalize the states corresponding to the vibration more than the rest of the states. Furthermore, the weight on the second input is smaller than the first input since the second motor has more authority in damping the vibrations out. The weighing matrices used in the cost function are

$$Q = \text{diag}(0.1I_{2 \times 2}, I_{2 \times 2}, 0.1I_{2 \times 2}, I_{2 \times 2})$$

$$R = \text{diag}(0.01, 0.0001).$$

The optimal solution over the linear output feedbacks is found through the optimization software and is given by

$$w_1 = \begin{bmatrix} -0.0652 \\ -9.4429 \end{bmatrix} y_1. \quad (48)$$

VI Simulation Results

A general purpose software for two-link planar manipulators with any number of modes was developed. The simulation studies to follow are for a two-mode model of a hybrid manipulator. The parameters of the models were chosen according to the experimental setup being developed at Control/Robotics Research Laboratory at Polytechnic University. We chose a larger length and a very flexible link not only to have a longer flexible arm (as the application motivates), but also to lower the vibrational frequencies and soften the link accordingly. The parameters of the manipulator are

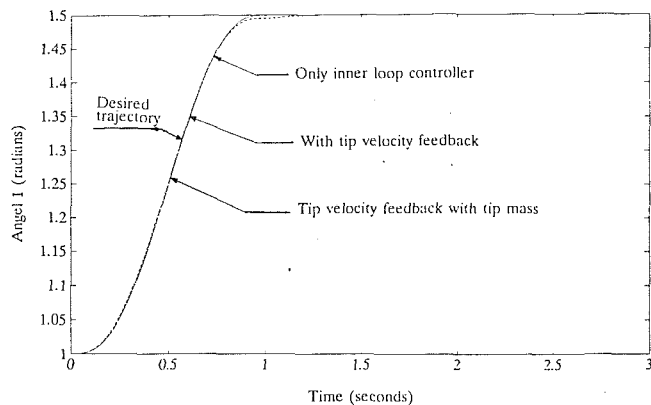


Fig. 4(a) The first joint angle, θ_1

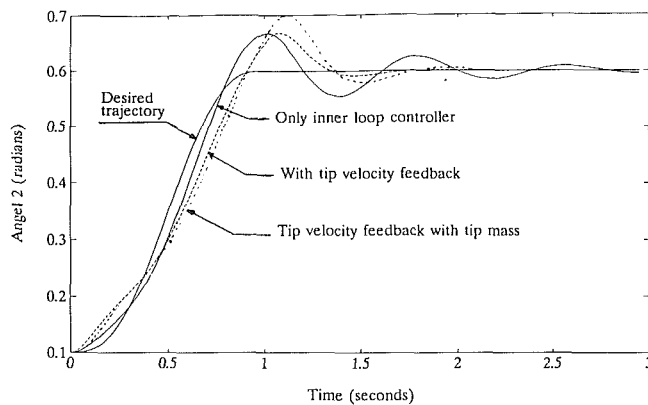


Fig. 4(b) The second joint angle, θ_2

Parameters of the links		
	Link 1	Link 2
EI	∞ (Rigid)	1.0 N-m^2
M	1.1	0.15 Kg
L	0.6	1.0 m
I_h	$8.47386 \times 10^{-1} \text{ Kg-m}^2$	0.0

The simulation results corresponding to the behavior of the manipulator under the inner-loop control action is depicted in Fig. 3. The simulations are for a fast large angle maneuver (i.e., thirty degree maneuver for each link in one second). The desired trajectories for the joint positions are generated by fifth degree polynomials. Although the vibrations are damped out at the end of the maneuver, the tracking performance during the whole interval is not satisfactory. The vibrations are even larger when the parameters are not exactly known by the controller. To contrast and compare the advocated inner-loop design to a simple joint-based controller, an independent joint PD control was applied. The gains of the PD controllers were chosen as $K_{i1} = 100$ and $K_{i2} = 20$ for both joints in all cases. The response of the system (i.e., joint angles and tip vibration) is depicted in the same figure (Fig. 3) for this PD controller. As can be observed, the vibrations are not only smaller for the nonlinear-based strategy, but also die out more quickly. To have a fair comparison, the gains were chosen to achieve the same speed of response.

Next, the tip velocity feedback was added as the outer-loop controller. In this case, the vibrations are much smaller as depicted in Fig. 4. In numerous simulations with different values for lengths and masses of the links in the controller we noticed a much better performance with the outer-loop in our feedback configuration. To verify the robustness of the advocated controller, the system is simulated with a payload mass. However, the same controller that was designed for the system with no payload was utilized. The payload mass chosen is 10 percent of the second-link mass. The simulation results are given in Fig. 4. Obviously, the vibrations are damped as before.

VII Conclusion

A complete description for modelling flexible-link manipulators was given. Furthermore, the distributed parameter model of a hybrid manipulator was derived. An inner-loop controller to feedback linearize the leading order term in the asymptotic expansion of the dynamics was employed. The gains in the inner-loop controller were chosen based upon the analytical expression derived for the vibration of the links through the asymptotic expansions.

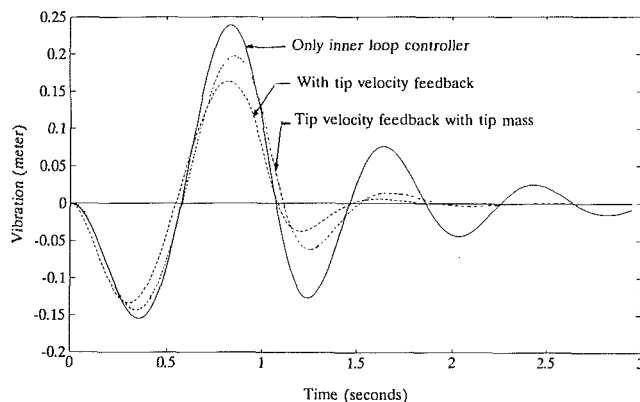


Fig. 4(c) Tip deflection, $\alpha_2(L_2, t)$

Fig. 4 Response of the arm under the inner/outer-loop controller

To further enhance the performance of the system and to enjoy robustness against parameter variations and unmodelled dynamics, an outer-loop controller was established through a linear quadratic design. The output required for the implementation of the outer-loop controllers can be obtained by accelerometers. It was shown that addition of the outer-loop improved the performance of the system considerably. It should be pointed out that the advocated technique is applicable to the multi-link flexible manipulators since the asymptotic expansions were derived for the multi-link case and the outer-loop controller is based upon a nonlinear non-convex optimization problem. The only difference in the multi-link case is the fact that a larger dimensional optimization problem need to be solved. This statement is not to minimize the difficulties one encounters in the experimental arena when the number of flexible links increase, but to establish a basis for theoretical tools available to approach the problem. The control methodology presented in the paper will go through if additional effects (e.g., axial displacement, torsion, etc.) are included in the dynamics of the manipulator. To further improve the response of the system, dynamic outer-loop compensators should be utilized. The aforementioned control algorithms will be implemented on our experimental setup in the future.

APPENDIX

A Finite-Dimensional Approximation of the Dynamics of Hybrid Manipulator

$$\mathcal{M} = \begin{bmatrix} m_{11} & m_{12} & m_{31} & \cdots & m_{i1} & \cdots \\ m_{12} & m_{22} & m_{32} & \cdots & m_{i2} & \cdots \\ \rho_2 < l_2, \Phi_1 > + \rho_2 L_1 C \theta_2 < 1, \Phi_1 > & \rho_2 < l_2, \Phi_1 > & \rho_2 L_2 & & 0 & \\ \rho_2 < l_2, \Phi_2 > + \rho_2 L_1 C \theta_2 < 1, \Phi_2 > & \rho_2 < l_2, \Phi_2 > & & \rho_2 L_2 & & \\ \vdots & \vdots & 0 & & \ddots & \\ \rho_2 < l_2, \Phi_p > + \rho_2 L_1 C \theta_2 < 1, \Phi_p > & \rho_2 < l_2, \Phi_p > & & & \rho_2 L_2 & \end{bmatrix}$$

$$\mathcal{K} = \begin{bmatrix} 0 & 0 & 0 & \cdots & \cdots & 0 \\ 0 & 0 & 0 & \cdots & \cdots & 0 \\ 0 & 0 & E_2 I_2 L_2 \lambda_1 & & 0 & \\ \vdots & \vdots & & E_2 I_2 L_2 \lambda_2 & & \\ \vdots & \vdots & 0 & & \ddots & \\ 0 & 0 & & & & E_2 I_2 L_2 \lambda_p \end{bmatrix}, F = \begin{bmatrix} f_1 \\ f_2 \\ \rho_2 L_2 (\dot{\theta}_1 + \dot{\theta}_2)^2 \eta_1 - \rho_2 L_1 < 1, \Phi_1 > \dot{\theta}_1^2 S \theta_2 \\ \rho_2 L_2 (\dot{\theta}_1 + \dot{\theta}_2)^2 \eta_2 - \rho_2 L_1 < 1, \Phi_2 > \dot{\theta}_1^2 S \theta_2 \\ \vdots \\ \rho_2 L_2 (\dot{\theta}_1 + \dot{\theta}_2)^2 \eta_p - \rho_2 L_1 < 1, \Phi_p > \dot{\theta}_1^2 S \theta_2 \end{bmatrix}$$

$$B = [I_{2,2} \mid 0 \dots 0]'$$

where m_{11} , m_{12} , m_{22} , f_1 and f_2 are as following:

$$m_{11} = I_h + \frac{1}{3} \rho_1 L_1^3 + \rho_2 L_1^2 L_2 + \frac{1}{3} \rho_2 L_2^3$$

$$+ \rho_2 L_1 L_2^2 C \theta_2 - 2 \rho_2 L_1 S \theta_2 \sum_{i=1}^p \eta_i < 1, \Phi_i > + \rho_2 L_2 \sum_{i=1}^p \eta_i^2$$

$$m_{12} = \frac{1}{3} \rho_2 L_2^3 + \frac{1}{2} \rho_2 L_1 L_2^2 C \theta_2$$

$$- \rho_2 L_1 S \theta_2 \sum_{i=1}^p \eta_i < 1, \Phi_i > + \rho_2 L_2 \sum_{i=1}^p \eta_i^2$$

$$m_{22} = \frac{1}{3} \rho_2 L_2^3 + \rho_2 L_2 \sum_{i=1}^p \eta_i^2$$

$$f_1 = \frac{1}{2} \rho_2 L_1 L_2^2 S \theta_2 (\dot{\theta}_2^2 + 2 \dot{\theta}_1 \dot{\theta}_2)$$

$$+ \rho_2 L_1 C \theta_2 (\dot{\theta}_2^2 + 2 \dot{\theta}_1 \dot{\theta}_2) \sum_{i=1}^p \eta_i < 1, \Phi_i >$$

$$+ 2 \rho_2 L_1 (\dot{\theta}_1 + \dot{\theta}_2) S \theta_2 \sum_{i=1}^p \dot{\eta}_i < 1, \Phi_i > - 2 \rho_2 L_2 (\dot{\theta}_1 + \dot{\theta}_2) \sum_{i=1}^p \eta_i \dot{\eta}_i$$

$$f_2 = -\frac{1}{2} \rho_2 L_1 L_2^2 S \theta_2 \dot{\theta}_1^2 - \rho_2 L_1 C \theta_2 \dot{\theta}_1^2 \sum_{i=1}^p \eta_i < 1, \Phi_i >$$

$$- 2 \rho_2 L_2 (\dot{\theta}_1 + \dot{\theta}_2) \sum_{i=1}^p \eta_i \dot{\eta}_i$$

References

- 1 Book, W. J., "Recursive Lagrangian Dynamics of Flexible Manipulator Arms," *International Journal of Robotics Research*, Vol. 3, No. 3, 1984, pp. 87-101.
- 2 Sunada, W., and Dubowsky, S., "On the Dynamic Analysis and Behavior of Industrial Robotic Manipulator with Elastic Members," *Trans. ASME*, Vol. 105, 1985.
- 3 Tarn, T. J., Bejczy, A. K., and Ding, X., "On the Modelling of Flexible Robot Arms," Tech. Rep. SSM-RL-87-08, Robotics Laboratory, Washington University, St. Louis, Missouri, Aug. 1987.
- 4 Low, K. H., "A Systematic Formulation of Dynamic Equations for Robot Manipulators with Elastic Links," *Journal of Robotic Systems*, Vol. 4, No. 3, 1987, pp. 435-456.
- 5 Khorrami, F., "Analysis of Multi-Link Flexible Manipulators Via Asymptotic Expansions," *Proceedings of the 28th Conference on Decision and Control*, Tampa, FL, Dec. 1989, pp. 2089-2094.

6 Cesareo, G., and Marino, R., "On the Controllability Properties of Elastic Robots," *Proc. 6th Int. Conf. Analysis Optimization Systems*, INRIA, (Nice, France), 1984.

7 Ding, X., Tarn, T. J., and Bejczy, A. K., "A Novel Approach to the Dynamics and Control of Flexible Robot Arms," *Proceedings of the 27th Conference on Decision and Control*, Austin, Texas, Dec. 1988, pp. 52-57.

8 Khorrami, F., "Dynamical Properties of Manipulators Exhibiting Flexibilities," *Proceedings of the IEEE International Conference on Systems Engineering*, Pittsburgh, PA, Aug. 1990, pp. 1-4.

9 Cannon, R. H., and Schmitz, E., "Initial Experiments on the End-Point Control of a Flexible One-Link Robot," *The International Journal of Robotics Research*, Vol. 3, No. 3, 1984, pp. 62-75.

10 Kotnik, P., Yurkovich, S., and Özgüner, Ü., "Acceleration Feedback for Control of a Flexible Manipulator Arm," *Journal of Robotic Systems*, Vol. 5, June 1988, pp. 181-196.

11 Hastings, G. G., and Book, W. J., "Verification of a Linear Dynamic Model for Flexible Robotic Manipulators," *Proceedings of the 3rd IEEE Int. Conf. Robotics and Automation*, (San Francisco, CA), Apr. 1986, pp. 1024-1029.

12 Barbieri, E., and Özgüner, Ü., "Unconstrained and Constrained Mode Expansions for a Flexible Slewing Link," *ASME JOURNAL OF DYNAMIC SYSTEMS, MEASUREMENT, AND CONTROL*, Vol. 110, Dec. 1988, pp. 416-421.

13 Krishnan, H., and Vidyasagar, M., "Control of a Single-Link Flexible Beam Using Hankel-Norm-Based Reduced Order Model," *Proceedings of the 5th IEEE International Conference on Robotics and Automation*, Philadelphia, Pa, Apr. 1988, pp. 9-14.

14 Lee, J., Huggins, J., and Book, W., "Experimental Verification of a Large Flexible Manipulator," *Proceedings of the 7th American Control Conference*, Atlanta, GA, 1988, pp. 1021-1028.

15 Bayo, E., "Computed Torque for the Position Control of Open-Chain Flexible Robots," *Proceedings of the 5th IEEE International Conference on Robotics and Automation*, Philadelphia, PA, Apr. 1988, pp. 316-321.

16 Oakley, C., and Cannon, R., "Initial Experiments on the Control of a Two-Link Manipulator with a Very Flexible Forearm," *Proceedings of the 7th American Control Conference*, Atlanta, GA, 1988, pp. 996-1002.

17 Schmitz, E., "Modeling and Control of a Planar Manipulator with an Elastic Forearm," *Proceedings of the 6th IEEE International Conference on Robotics and Automation*, Scottsdale, Arizona, Apr. 1989, pp. 894-899.

18 Khorasani, K., and Spong, M. W., "Invariant Manifold and Their Application to Robot Manipulators with Flexible Joints," *IEEE Proceedings*, 1985, pp. 978-983.

19 Spong, M. W., Khorasani, K., and Kokotovic, P. V., "An Integral Manifold Approach to Feedback Control of Flexible Joint Robots," *IEEE Journal of Robotics and Automation*, Vol. RA-3, Aug. 1987, pp. 291-300.

20 Siciliano, B., and Book, W. J., "Singular Perturbation Approach to Control of Lightweight Flexible Manipulators," *The Int. Journal of Robotics Research*, Vol. 7, Aug. 1988, pp. 79-90.

21 Khorrami, F., and Özgüner, Ü., "A Singular Perturbation Analysis of a Distributed Parameter Model of Flexible Manipulators," *Proceedings of the 7th American Control Conference*, Atlanta, Georgia, June 1988, pp. 1704-1709.

22 Meirovitch, L., *Analytical Methods in Vibrations*, The MacMillan Company, New York, 1967.

23 Khorrami, F., "Asymptotic Expansions in Analysis of Multi-Link Flexible Manipulators," Tech. Rep. CRR-1001-10/88-P, Control/Robotics Research Laboratory, Polytechnic University, Brooklyn, NY, 1988.